

# RSC Advances



This is an *Accepted Manuscript*, which has been through the Royal Society of Chemistry peer review process and has been accepted for publication.

*Accepted Manuscripts* are published online shortly after acceptance, before technical editing, formatting and proof reading. Using this free service, authors can make their results available to the community, in citable form, before we publish the edited article. This *Accepted Manuscript* will be replaced by the edited, formatted and paginated article as soon as this is available.

You can find more information about *Accepted Manuscripts* in the [Information for Authors](#).

Please note that technical editing may introduce minor changes to the text and/or graphics, which may alter content. The journal's standard [Terms & Conditions](#) and the [Ethical guidelines](#) still apply. In no event shall the Royal Society of Chemistry be held responsible for any errors or omissions in this *Accepted Manuscript* or any consequences arising from the use of any information it contains.

## ARTICLE

# Nanostructured and Spiky Gold in Biomolecule Detection: Improving Binding Efficiencies and Enhancing Optical Signals

Cite this: DOI: 10.1039/x0xx00000x

Received 00th January 2012,  
Accepted 00th January 2012

DOI: 10.1039/x0xx00000x

www.rsc.org/

E.E. Bedford,<sup>a,b,c,d</sup> S. Boujday<sup>a,b</sup>, C-M. Pradier<sup>a,b</sup> and F.X. Gu<sup>c,d</sup>,

Nanostructured gold can improve the ability to detect biomolecules. Whether planar nanostructured surfaces or nanostructured particles are used, similar principles governing the enhancement apply. The two main benefits of nanostructured gold are improved geometry and enhancement of optical detection methods. Nanostructuring improves the geometry by making surface-bound receptors more accessible and by increasing the surface area. Optical detection methods are enhanced due to the plasmonic properties of nanoscale gold, leading to localized surface plasmon resonance sensing (LSPR), surface-enhanced Raman scattering (SERS), enhancement of conventional surface plasmon resonance sensing (SPR), surface enhanced infrared absorption spectroscopy (SEIRAS) and metal-enhanced fluorescence (MEF). Anisotropic, particularly spiky, surfaces often feature a high density of nanostructures that show an especially large enhancement due to the presence of electromagnetic hot-spots and thus are of particular interest. In this review, we discuss these benefits and describe examples of nanostructured and spiky gold on planar surfaces and particles for applications in biomolecule detection.

## Introduction

From medicine to environmental monitoring to food contamination protection, detection of biomolecules (such as bacteria, DNA, or proteins) helps to protect our health and environment. Over the past two decades, biosensor research has taken off, inspired by the success of the hand-held glucose sensors used by diabetic patients, but expanding into the detection of all types of biomolecules using a variety of transduction methods.<sup>1</sup> No matter the method of detection, high sensitivity is one of the constant goals within the field of biosensor research. Since many methods involve concentrating biomolecules on a surface for signal transduction, a key strategy to achieve high sensitivities is to optimize the surfaces on which probes are bound so that a large number of analyte molecules can be bound and a sufficiently strong signal produced.

Affinity-based biosensors harness the specific affinity between certain biomolecules to detect the presence and quantity of a biomolecule. These make use of the same interactions that allow for currently used methods of detecting biomolecules such as immunoassays, which make use of the affinity between antigens and antibodies (ELISA, for example), and hybridization assays, which make use of the affinity between complementary nucleic acid strands (Southern and northern blot assays, for example). By using affinity interactions to

specifically bind an analyte of interest—typically on a solid surface—they can be detected by various methods of signal transduction (Figure 1). Biomolecules are small, so harnessing their specific interactions requires tools of a comparable scale—a job that nanostructured gold fills well; gold is biocompatible, chemically stable, and can easily be functionalized.<sup>2-5</sup>

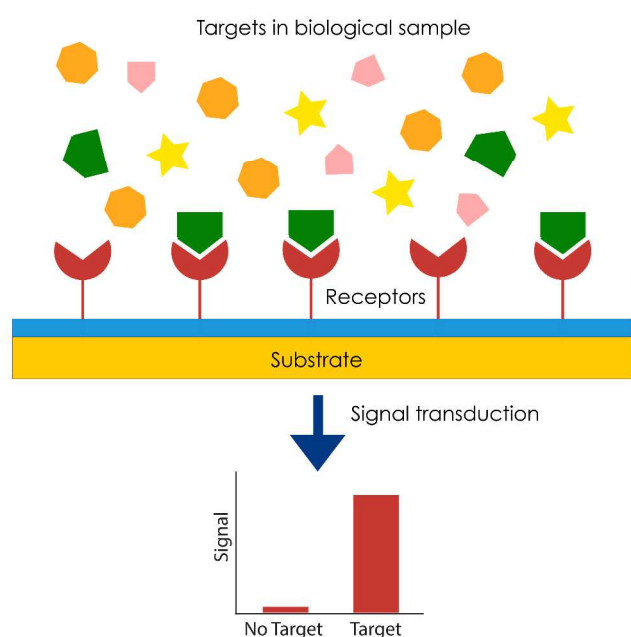


Figure 1: General scheme of biosensors. Targets in a biological sample bind to receptors bound to a substrate. Signal transduction indicates target binding

While electrochemical methods have traditionally been the most commercially successful biosensing methods, optical detection methods have also proved interesting by offering highly sensitive, label-free detection—a primary example being the prevalence of surface plasmon resonance (SPR) detection in R&D.<sup>1</sup> Optical methods of detection make use of changes in the optical signal—absorption, luminescence, fluorescence, and plasmon resonance, for example—that occur upon binding. Again, nanostructured gold stands out as an interesting material, in this case, because of its interesting optical properties. Surface plasmons can be excited in metallic nanoparticles by specific wavelengths of light due to the confinement of electrons within the small particles.<sup>6,7</sup> In gold nanoparticles, this surface plasmon resonance (SPR) frequency is in the visible range, leading to the characteristic red colour of gold nanospheres and other colours in gold nanoparticles of different shapes and sizes. In addition to these distinct colours, the confined surface plasmons lead to enhanced electromagnetic fields at the particle surfaces. Anisotropic shapes, such as “spiky” tips, lead to particularly strong enhancements, often referred to as electromagnetic hot-spots.<sup>6,8-11</sup> In localized surface plasmon resonance (LSPR) sensing, biomolecule binding leads to a shift in gold nanoparticle absorbance, which is larger when biomolecules are bound to hot-spots compared with other areas of the gold nanoparticle surface.<sup>12-15</sup> Other methods of optical detection, such as surface-enhanced Raman scattering (SERS),<sup>8,16,17</sup> surface enhanced infrared absorption spectroscopy (SEIRAS),<sup>8,18,19</sup> and metal-enhanced fluorescence (MEF)<sup>20</sup> also show an enhanced signal due to this hot-spot phenomenon that can be harnessed for biosensing applications.

Extraordinarily innovative methods have been used to form spiky gold nanostructures that exhibit the above features.

Methods like electron beam lithography and atomic force microscopy can make precise structures that are extremely useful in studying the above phenomena, but the practical harnessing of these phenomena in biosensing likely requires simpler methods of nanostructure formation that can be done on a larger scale or that are more accessible to non-specialized laboratories.

In this review, we first discuss the benefits of using nanostructured gold—specifically, the improved binding efficiencies and enhanced optical signals that can result—followed by a (non-exhaustive) look at examples of methods used to nanostructure gold surfaces with a focus on chemical methods and those requiring less specialized equipment.

## 50 Benefits of Nanostructuring

Recent work has shown that there are numerous benefits to nanostructuring surfaces, including geometric benefits involving the position, orientation, and accessibility of immobilized biomolecules as well as enhancement of optical transduction methods. Our focus in this review will be on the geometric benefits and the enhancement of optical detection methods using nanostructured gold. This covers two different methods of enhancement: geometric optimization, by increasing the number of targets available for detection, and optical detection method enhancement, by increasing the sensitivity of the technique to a single recognition event.

### Geometric Benefits

#### NUCLEIC ACIDS

DNA biosensors use the specific interaction between complementary strands of DNA bound to a surface and the DNA molecules of interest to detect the presence of a particular DNA sequence. Hybridization with DNA probes bound to a surface introduces new challenges compared with standard hybridization in solution. Hybridization efficiencies are reduced by electrostatic repulsion and steric hindrance between immobilized strands, and by non-specific adsorption of oligonucleotides to the surface.<sup>21-24</sup>

The idea that working with small biomolecules requires small tools has led to much research on the differences that occur between binding oligonucleotides to nanostructured surfaces and binding to planar ones. In particular, the surface curvature influences the interactions between bound probes, and consequently, the number of probes that can be immobilized on a surface. Researchers have found that the loading density of thiolated DNA strands on sufficiently curved gold surfaces (for spherical particles, this means having a diameter less than 60 nm) can be an order of magnitude larger than on planar surfaces.<sup>25,26</sup> This may be due to decreased electrostatic repulsion due to increased deflection angles between strands on smaller particles.<sup>25,26</sup> This theory is supported by the fact that loading density also depends on salt concentration, where an increase in salt concentrations, up to a point, results in

increased loadings due to its neutralizing effects on the negatively charged phosphate backbone of DNA.

While DNA loading is increased on curved surfaces, whether the highest possible DNA probe loading also results in optimal DNA hybridization is another question. While high DNA probe loadings are important in ensuring that a high number of targets are bound to a surface through hybridization, steric and electrostatic issues also become factors. On planar surfaces, optimal probe coverage for target binding involves a balance between a high number of probes for targets to be bound to a low enough density that steric and electrostatic issues are not a problem. Several groups have shown that high probe densities reduce hybridization efficiencies.<sup>21-23</sup> Irving et al demonstrated that the reduction in hybridization efficiencies that results with high probe densities can be divided into regimes based on the main mechanism of hybridization suppression: an electrostatic suppression regime at lower salt concentrations and a packing suppression regime at higher salt concentrations.<sup>22</sup>

Do the same crowding issues occur on non-planar surfaces? We know that curved surfaces result in increased deflection angles between immobilized strands, so it would be expected that immobilization on convex surfaces at the same “footprint” densities as on planar surfaces would result in greater spacing between the accessible ends of strands, thus reduced electrostatic and steric barriers. This phenomenon has, in fact, been demonstrated experimentally. The Kelley lab demonstrated that detection limits are decreased by several orders of magnitude when electrochemically detecting DNA hybridization on nanostructured palladium<sup>27-29</sup> or gold<sup>30-32</sup> compared with smooth metal surfaces. Their work supported the hypothesis that the enhancement is caused by favorable geometries for hybridization (**Figure 3**) by showing that the greatest enhancements occur with fine nanostructuring (20-50 nm)—a similar length scale to the immobilized oligonucleotides (5-10 nm)<sup>29</sup>—and by showing that higher hybridization efficiencies occurred on nanostructured surfaces even after surface area normalization.<sup>28</sup>

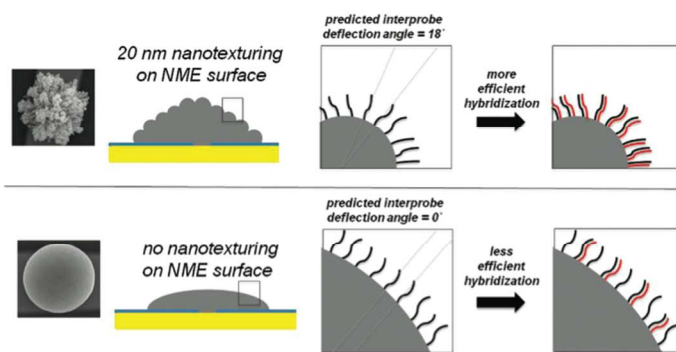


Figure 3: Proposed model of the effect of nanostructuring on DNA binding and hybridization. Nanostructured microelectrodes (NMEs) were used for electrochemical detection of DNA hybridization with and without nanotexturing. Reprinted with permission from ref<sup>28</sup>. Copyright 2010 American Chemical Society.

Other researchers have also demonstrated improved surface hybridization efficiencies due to nanostructured surfaces.<sup>2</sup> Enhancement of electrochemical DNA hybridization sensors has been shown using dendritic gold nanostructures,<sup>33</sup> gold nanoflower-like structures,<sup>34</sup> gold-nanoparticle coated surfaces,<sup>35</sup> other roughened gold surfaces,<sup>35,36</sup> and chemical nanostructuring and sub-nanometer structuring using mixed self-assembled monolayers (SAMS).<sup>37</sup>

As we can see, much of the work to date involving harnessing the geometric benefits of nanostructured surfaces on DNA hybridization has involved electrochemical sensors. There is good reason to believe, though, that it would exhibit enhancements in other detection methods as well, such as optical or piezoelectric-based transduction methods, since increasing the number of species bound will increase the signal of any quantitative or semi-quantitative method.

#### PROTEINS

Like nucleic acids, the surface adsorption of proteins is influenced by surface nanostructuring. Unlike nucleic acids, proteins often exhibit a number of functional sites that can be bound to a surface, making control over their binding orientation both more difficult and more critical for subsequent recognition. For example, in immunosensing, involving recognition between an antibody and its corresponding antigen, it is required that the antibody be immobilized on a surface in an orientation that leaves the antigen binding site (Fab fragment) accessible.<sup>38</sup> It is also critical to avoid protein denaturation or conformational changes when binding proteins to a surface.<sup>39-41</sup> There are a number of methods that can be used to do this, as discussed already in a number of publications.<sup>38,39,42,43</sup> In addition to immobilization in the proper orientation, it is important to ensure that the density of bound proteins does not interfere with recognition ability. High protein densities on the surface can block the active sites of antibodies or other protein probes, preventing antigen binding.<sup>42,44</sup>

Surface nanostructuring can be a good way to ensure suitable binding densities and protein spacing. Work involving differently nanostructured arrays prepared by AFM nanografting of SAMs demonstrates the dependence of protein binding density and local environment on subsequent protein recognition; when arrays were designed according to the size of antibodies Fab sites, greater antibody recognition occurred<sup>45</sup> (proposed model in **Figure 4**). A number of methods have also successfully been used to increase recognition efficiencies, including mixed SAMs giving chemically nanostructured surfaces,<sup>45-47</sup> the use of dendrimers to create nanoscale spacing between SAMs containing active groups,<sup>48</sup> and nanostructured surfaces created by nanoparticle deposition.<sup>49-51</sup>

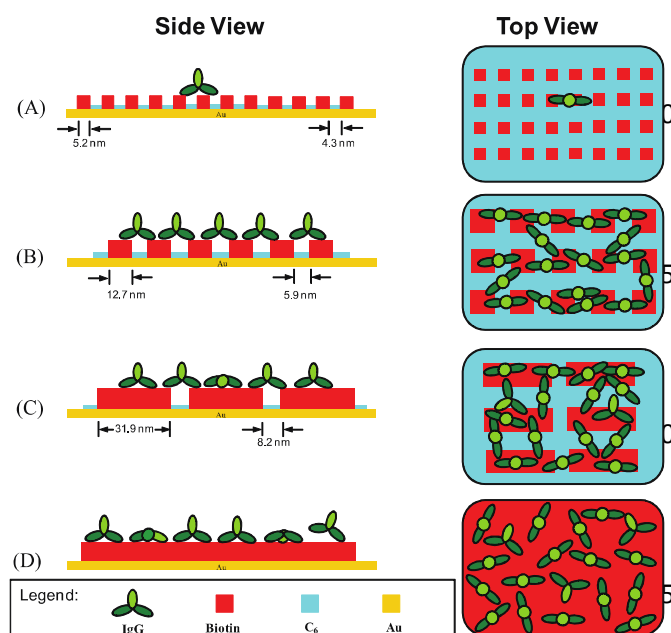


Figure 4: Proposed model of the effect of nanostructuring on protein-antibody (biotin-IgG) interactions. Feature sizes similar to the size of the binding domains of IgG result in higher recognition (B, C). Feature sizes that are too small prevent recognition (A) and those that are too large result in random orientations (D). Reprinted with permission from ref<sup>45</sup>. Copyright 2008 American Chemical Society.

Another benefit of nanostructuring is an increased surface area available for probe binding. Rusling's group claims this to be a contributing factor to the extremely low detection limits achieved in their electrochemical immunosensors featuring nanostructured surfaces using gold nanoparticles.<sup>50,51</sup> The effects of these two contributing mechanisms of enhancement—optimal protein density and increased surface area—can be difficult to separate, but the existing literature suggests that both play role in increasing analyte binding.

### Enhancement of Optical Detection Methods

The plasmonic properties of gold surfaces and nanostructures have made them a major focus in current diagnostics research. Surface plasmons are electron cloud oscillations that occur at the boundary between a metal and a dielectric. Waves of surface plasmons, known as surface plasmon polaritons, can be excited by photon or electron irradiation. Surface plasmon resonance (SPR) sensing makes use of changes related to these surface plasmon waves due to analyte binding for sensing applications including food quality and safety analysis, medical diagnostics, environmental monitoring, and drug discovery.<sup>52,53</sup> In the case of nanosized and nanostructured materials, the surface plasmon polariton is confined to a small area, smaller than the wavelength of the incident light, resulting in a phenomenon called localized surface plasmon resonance (LSPR). The wavelength for LSPR depends, among other factors, on the size of the nanostructure; when excited, it leads to enhanced light absorption and scattering. When these types of structures are used as substrates in techniques involving light absorption and scattering, such as Raman and infrared

spectroscopy and fluorescence detection, they can electromagnetically enhance the detection signal, leading to phenomena such as surface-enhanced Raman scattering (SERS), surface-enhanced infrared absorption (SEIRA), and metal-enhanced fluorescence (MEF). Another related phenomenon involves electromagnetic hot-spots created at sharp tips and in small spaces between nanostructures—nanogaps—that can enhance optical processes, further increasing the enhancements seen in SERS, SEIRA, and MEF.<sup>8-11</sup> While all related phenomena have been used, both independently and simultaneously in interesting biosensing methods, the focus in this work regarding enhancement of optical methods will be on methods that make use of the latter phenomena—the creation of electromagnetic hot-spots and their use in diagnostic applications.

Several other reviews cover the general topic of optical enhancement by nanomaterials for biomedical applications in more detail.<sup>2,54,55</sup>

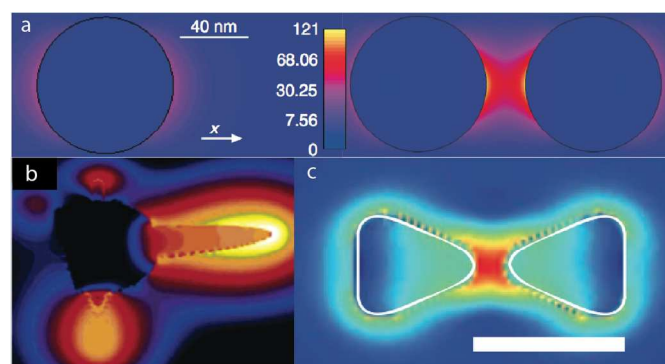


Figure 5: Simulations of electromagnetic enhancement at a) nanogaps<sup>56</sup>, b) sharp tips<sup>57</sup>, and c) combined sharp tips and nanogaps (bowtie nanoantenna)<sup>58</sup>.

### LSPR SENSORS

Localized surface plasmon resonance (LSPR) sensors offer some of the simplest set-ups in terms of optical methods making use of nanostructured surfaces. Sensing can require as little as the human eye, as is the case for colorimetric biosensing, or for more sensitive detection, a UV-visible spectrometer. LSPR sensing involves detecting changes in the refractive index, due to analyte binding, for example; a change in the refractive index causes changes in the frequencies needed for surface plasmon resonance. The greatest changes occur when binding occurs at electromagnetic hot-spots, such as nanogaps and sharp tips.<sup>12-14</sup>

A number of different formats have been used in LSPR sensing. Most LSPR sensors can be divided into either aggregation sensors or refractive index sensors.<sup>9</sup> In aggregation sensors, analyte presence induces metal nanoparticle aggregation, which results in a shift in the plasmonic peak of the particles.<sup>59-61</sup> In refractive index sensors, analyte presence induces a change in the refractive index of the dielectric medium at the surface of the metal, which also results in a plasmonic peak shift. A change in the refractive index at an electromagnetic hot-spot

5 results in especially large shifts. A recent review names<sup>55</sup> preferential binding to these hot-spots as the next step in LSPR research,<sup>54</sup> and to date, some researchers have demonstrated hot-spot enhancement by preferentially binding biomolecules to hot-spot structures. Beeram and Zamborini demonstrated this by selectively binding anti-IgG to the edges of gold nanostructures on planar surfaces; the limit of detection when anti-IgG was selectively bound to electromagnetic hot-spots was at least 500 times lower than when not bound selectively.<sup>12</sup> 10 Feuz et al also demonstrated this by selectively binding proteins to the hot-spot between two nanodisks and comparing the signal with binding to single gold disks. When normalized for surface area and thus signal per molecule, the signal is greater in nanogaps than on entire disks.<sup>13</sup>

## 15 SPR SENSORS

Surface plasmon resonance (SPR) sensors detect changes at a metal-dielectric interface by measuring changes in the conditions required to excite surface plasmons.<sup>53</sup> Previous work has shown that combining planar gold surfaces with plasmonic nanostructures can result in stronger signals and higher sensitivities.<sup>52</sup> The enhancement is thought to be due to coupling between surface plasmon polaritons (SPP) of the planar surface and localized surface plasmon resonance (LSPR) of the nanostructures.<sup>62,63</sup> While the greatest improvements have been seen using gold nanostructures as labels<sup>62,64-69</sup> (as the presence or absence of coupling is dependent on analyte binding), modest improvements have also been observed when gold nanoparticles are incorporated into the substrate.<sup>63,70-75</sup> Nano- and micro-hole arrays offer another example of this coupling phenomenon.<sup>76</sup> Holes in gold surfaces produce localized plasmons (similar to the nanogap enhancement observed between particles) and these are coupled with surface plasmons that propagate across the sample surface.

## SERS

35 Surface-enhanced Raman scattering, widely known as SERS, uses electromagnetic fields in metallic nanostructures to enhance the intensity of the signal in Raman spectroscopy. SERS results in a signal enhancement of many orders of magnitude, inspiring many potential applications due to fingerprint specificity. In the case of biosensing applications, detection could involve directly measuring the spectra of the analyte, but more often, detection involves measuring the spectra of a Raman reporter molecule combined with a metallic nanostructure; the fingerprint specificity of Raman spectroscopy allows a multiplexing approach through the use of different reporter molecules. Much of the enhancement due to metallic nanostructures is thought to be because of electromagnetic enhancements caused by SPR. To briefly discuss, incident light excites surface plasmons, creating a strong electromagnetic field on the surface. The Raman modes of molecules close to the surface are consequently enhanced. Further enhancement occurs when the Raman mode is the same as the plasmon resonance wavelength. Chemical enhancement based on the interaction between bound molecules and

metal surface is also thought contribute to the observed enhancement.<sup>16,77</sup>

Many different structures and set-ups have been used for SERS, ranging from the initial discovery of the phenomenon using a roughened silver electrode,<sup>78</sup> to spherical and anisotropic nanoparticles free in solution or deposited on surfaces, to periodic arrays of metal nanostructures.

Based on numerous experimental and theoretical studies, evidence suggests that the electromagnetic field enhancement needed for SERS is particularly prominent in two general types of nanostructures: nanogaps and sharp tips, together called hot-spots. Nanogaps as hot-spots are commonly seen when using solution-based SERS, using metallic (usually gold or silver) nanoparticles<sup>8,79,80</sup>. The SERS intensity varies with interparticle distance and is greatest when the particles are close together; both experimental and theoretical demonstrations of dimer plasmons show this phenomenon.<sup>11,81-84</sup> Nanostructures with sharp tips feature strong electromagnetic enhancement at the tip.<sup>10,85,86</sup> The SERS signal of molecules bound at or near the tips can be enhanced by many orders of magnitude.<sup>87</sup> Gold nanostars, featuring a sphere-like core and branches of various numbers and sizes, are often investigated for this purpose.<sup>10,57,88,89</sup>

One of the main challenges in SERS is reproducibility of the substrate. Small changes in the substrate, such as the size of or distance between nanostructures, result in large changes in signal, which makes the synthesis of reproducible substrates challenging. As this continues to be a hurdle in bringing SERS into more general use, the reproducibility issues are discussed in detail in other reviews.<sup>16,90</sup> While extremely high SERS enhancement has been shown—as high as  $10^{14}$  for single molecule measurements—these enhancements can be attributed to the hot-spot phenomenon, occurring in only a small part of a measurement. When measurements are averaged over a larger area and time, enhancements tend to be on the order of  $10^4$  to  $10^7$ .<sup>16</sup> Nanoparticle solution-based methods often suffer from low reproducibility as the presence of hot-spots requires the molecule of interest to be in a nanogap between two or more particles; well-dispersed sols therefore often show weak SERS signals.<sup>90</sup> A common method is to deposit the sol on a solid substrate, which results in much greater enhancements, but still suffers from reproducibility issues due to surface inhomogeneity.<sup>16</sup>

Using SERS substrates that make use of a sharp tip hot-spot can avoid some of these reproducibility issues resulting from the difficulty in ensuring molecules are trapped within nanogaps. Rather than immobilizing molecules in gaps between gold nanostructures, molecules can be immobilized on anisotropic surfaces. A common example of this is the use of gold nanostars for SERS. Nordlander's group modeled gold nanostars by the finite-difference time-domain method, showing that the tips generate electromagnetic field enhancements that are increased by the nanostar core, which acts like a nanoscale antenna; the resulting plasmons thus result from hybridization of the core and tip plasmons.<sup>57</sup> Gold nanostars show greater SERS signals than spherical gold

nanoparticles due to this tip-based enhancement, without the need for particle aggregation to create nanogaps.<sup>10,89,91,92</sup>

### SEIRAS

Surface enhanced infrared absorption spectroscopy (SEIRAS) is another example of nanostructured metals providing electromagnetic enhancement. The effect is similar to SERS but with enhancement occurring in the mid-infrared region and lower enhancement factors compared with SERS, on the order of 10 to 10<sup>3</sup>.<sup>18,19</sup> As in SERS, nanostructured metals lead to greater enhancements, although the type of nanostructures and mechanism of enhancement differs.<sup>93</sup> Substrates that exhibit both SERS and SEIRAS—gold nanoshells, for example—can allow for the complementary use of both techniques.<sup>8,93</sup>

### MEF

Fluorescent labels are the most common labels used in the life sciences for detection of biomolecules. Increasing the signal intensity of these methods would be of definite benefit. Metal enhanced fluorescence (MEF) makes use of the plasmon properties of metal nanostructures to amplify the light emitted by fluorophore excitation. In addition to increasing the quantum yield of fluorophores, metal nanostructures can also improve the photostability of fluorophores.<sup>20,94</sup> As observed in other optical detection methods, fluorophore binding to electromagnetic hot-spots results in signals orders of magnitude greater than without electromagnetic enhancement.<sup>95-97</sup>

## Types of Gold Nanostructuring

There are an extraordinary number of methods that can be used to create gold nanostructured surfaces. Nanomaterial synthesis is traditionally divided into bottom-up or top-down techniques, where bottom-up refers to building nanomaterials from smaller components and top-down refers to building nanomaterials using larger equipment to etch or deposit nanoscale features. The emphasis in this paper will be on bottom-up approaches to gold nanostructuring and hot-spot formation, which tend to take inspiration from classical chemical synthesis and less often require specialized equipment.

Different methods of biosensing will benefit from different types of surfaces. While biosensors using nanoparticles in solution have the benefit of large surface areas, planar surfaces often offer better control over signal reproducibility. In all cases, compatibility with the sensing method is the deciding factor.

### Planar Surface Nanostructuring

#### SELF-ASSEMBLED MONOLAYERS

“Self-Assembled Monolayers of Thiolates on Metals as a Form of Nanotechnology”, a well-known review by Love et al of the Whitesides group,<sup>98</sup> excellently describes how self-assembled monolayers—SAMs—can be involved in nanostructuring surfaces. SAMs have become a necessary tool in biosensor research, with uses that include both enabling interaction

nanostructured surfaces with biomolecules and creating nanostructured domains of functional groups that can be used to selectively bind nanostructures or biomolecules directly.

Self-assembled monolayers of alkanethiols are commonly used for biomolecule attachment on sensor surfaces because they can easily be formed and their functionality can be easily controlled by choosing suitable alkanethiol head groups. By using, for example, amine or carboxylic acid head groups, proteins can be covalently bound to SAMs on gold surfaces.

On crystalline surfaces under controlled vacuum conditions, well-ordered SAMs form in which the molecules align due to van der Waals interactions between the hydrocarbon backbones.<sup>98,105</sup> On surfaces featuring deviations from perfect crystallinity—through defects or intentional nanostructuring—chains have been shown to align differently, further enhancing how a defect is “seen” by a biomolecule. Polycrystalline gold surfaces are common substrates for biosensing applications; alkanethiolate SAMs on these surfaces show areas of order and disorder, with areas of disorder often corresponding to areas of gold grain boundaries, impurities, and defects such as steps and vacancies.<sup>98</sup>

For certain applications, the defects can be harnessed and used to their advantage. Place exchange reactions occur more easily in these areas of disorder because of lower intermolecular interactions, allowing for chemical nanostructuring by controlling areas of order and disorder of the substrate.<sup>98,106</sup> Defects can also result in “cage-like” sites, meaning that a biomolecule at a defect will encounter a geometry allowing it to contact more functional groups at once.<sup>103</sup>

Research involving alkanethiol monolayers on gold has shown that when two or more different alkanethiols are used (different head group or alkane chain), rather than creating monolayers with an even distribution of alkanethiols, they tend to phase separate and, under certain conditions, form nanostructured domains. While precise control is difficult, the average size and number of these nanostructured domains can be controlled by changing the ratio between components in the deposition solution.<sup>107,108</sup>

The size of these nanostructured domains is often similar to the size of many proteins (10-50 nm<sup>2</sup>), which makes them interesting in biosensing applications where control over biomolecule density and prevention of non-specific binding are important factors.<sup>102,109-111</sup> Mixed monolayers can also include diluting thiol-tagged oligonucleotides with an alkanethiol that prevents non-specific binding and increases spacing between bound DNA strands for hybridization-based sensing.<sup>112-114</sup>

When more precisely defined domains are desired, SAMs can be patterned using classic nanotechnology methods, such as using AFM for dip-pen nanolithography or nanografting, soft lithography methods like microcontact printing, or patterning using energetic beams.<sup>45,47,98,106</sup>

In addition to linking biomolecules to gold surfaces, SAMs are also used to link nanostructures synthesized separately and planar surfaces, as shown by several of the examples given in the following section.

## NANOPARTICLE AND LARGE MOLECULE BINDING

When nanostructures involving more than just nano-sized domains of functional groups are desired, a common method is to bind previously synthesized nanostructures to the surface.

- 5 Nanostructures at similar scales to the biomolecule of interest can help control the biomolecule density. When the nanostructures are gold or another plasmonic material, they can also exhibit plasmonic enhancement effects.
- 10 Many researchers have investigated gold nanoparticles bound to gold surfaces primarily for the potential optical detection enhancement that can arise.<sup>50,51,115,116</sup> These surfaces have shown SPR enhancement which is the subject of a previous review.<sup>52</sup> The quest for reproducible SERS substrates is another application of this type of nanostructured gold surface. In this case, the goal is controlled spacing—or at least controlled average spacing—between gold nanoparticles to avoid the issues of reproducibility that plague the SERS literature. Strategies to achieve this include binding the nanoparticles to groups on a gold or other surface (often  $-SH$  or  $-NH_2$ ).<sup>117</sup> The average interparticle spacing can be controlled by the nanoparticle concentration, deposition time, and other experimental factors. When averaged over a large enough laser spot size, the resulting signal can be reproducible. Very monodisperse nanoparticles will even assemble into ordered arrays with small, controlled spacing between particles that can be tuned by varying the length of stabilizing molecules.<sup>79,118</sup>

- 25 Other molecules on the same size scale as biomolecules can also be used to nanostructure surfaces. The primary goal in this case is for geometrical considerations—controlled spacing between biomolecules. Researchers have made nanostructured surfaces using dendrimers,<sup>48,119</sup> polyoxometalates,<sup>120</sup>  $TiO_2$  nanoparticles,<sup>49</sup> and carbon nanotubes.<sup>121</sup>

## NANOSPHERE LITHOGRAPHY

- 35 Unlike the previously discussed approaches, nanosphere lithography is a top-down approach to nanostructuring, but one that is more easily applied in a non-specialized laboratory than traditional lithography techniques. In nanosphere lithography, a layer of near-monodisperse nanospheres is deposited on a substrate and used as a mask for further deposition or etching steps (Figure 6). Under the right conditions, the nanospheres will form an ordered array. The Van Duyne group first introduced this method in 1995<sup>122</sup> using a polystyrene nanosphere array as a mask for evaporated metal, forming nanotriangles. Later work uses the same method to prepare silver nanotriangle arrays of controlled size and spacing for LSPR<sup>123</sup> and SERS<sup>124</sup> sensing surfaces. The size and shape of the formed nanostructures can be varied by changing the size and number of layers of nanospheres used to form the mask.

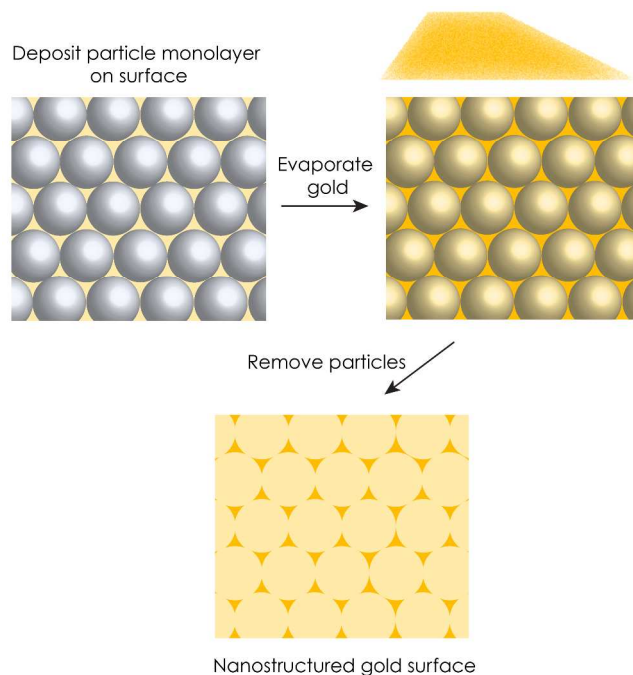


Figure 6: General scheme of nanosphere lithography

## ELECTROCHEMICAL DEPOSITION

Electrochemical deposition of nanostructures on planar gold electrodes has resulted in biosensing surfaces with high sensing efficiencies.<sup>33,36</sup> Applying a potential to the electrode in the presence of a gold salt solution results in various morphologies of gold nanostructures (Figure 7). Using a similar method but with platinum instead of gold, the Kelley group was able to control the size of nanostructures on electrodes, and demonstrated that finer nanostructuring resulted in higher hybridization efficiencies of oligonucleotides.<sup>28,29</sup> In biosensing, this method has most often been used with electrochemical sensors where only geometrical enhancement plays a role, but in other areas, electrochemically deposited surfaces have proven to also provide optical enhancement, in their use as SERS substrates for example. Researchers synthesized dendritic gold structures<sup>125</sup> and nanoflowers<sup>126</sup> using electrochemical deposition and were able to detect rhodamine 6G at concentrations as low as  $10^{-12}$  M. Another approach used a mask similar to that used in nanosphere lithography to synthesize organized nanoflower arrays by electrodeposition and also exhibited SERS enhancement.<sup>127</sup> Gold deposited in this way likely exhibits multiple hot-spots at the tips of the structures<sup>125</sup> as well as in nanogaps between the structures.<sup>127</sup> It may be of interest to further investigate the use of electrochemically synthesized gold nanostructures as templates for biomolecule detection using optical methods like SERS.

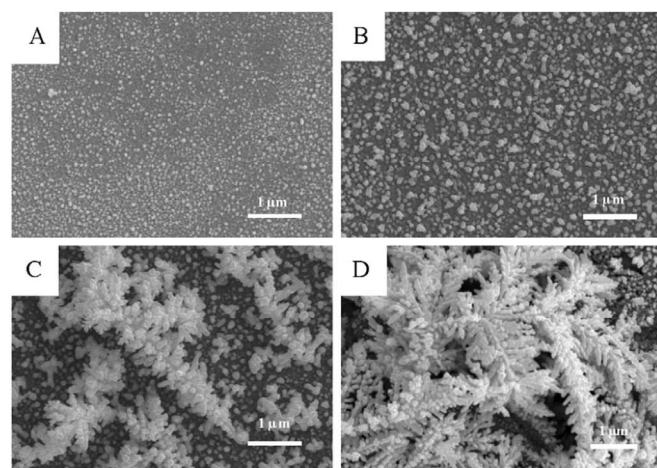


Figure 7: SEM images of gold nanostructured surfaces formed by electrodeposition for different times: (A) 20 s, (B) 100 s, (C) 300 s, and (D) 600 s.<sup>33</sup>

## 5 Particle Nanostructuring

### ANISOTROPIC GOLD NANOPARTICLES

Easily the most well known form of nanostructured gold used in biosensing applications is the gold nanoparticle. Gold sols have been used in various forms for centuries,<sup>128</sup> but only in the past half a century has their use in diagnostics been investigated. As the main interest lies in exploiting their size-dependent optical properties, the ability to synthesize controlled, monodisperse, stable sols is critical to their use. The most commonly used methods of synthesis involve reduction of a gold salt in the presence of a stabilizing ligand; citrate reduction of HAuCl<sub>4</sub> is useful when a loose shell of ligands is desired, and the Brust-Schiffrin method, using thiols as stabilizing ligands, is useful when more monodisperse and stable particles are needed.<sup>129,130</sup>

More recently, interest in nonspherical gold nanoparticles has grown, largely due to the interesting optical phenomena they exhibit. Gold nanorods, nanostars, nanocubes and other particles of different shapes and sizes (see Dreaden et al<sup>5</sup> for further examples) often feature multiple plasmon bands and bands that reach into NIR wavelengths. These alternative shapes, particularly those with high aspect ratio features like nanostars, can result in electromagnetic hot-spots that can enhance optical signals (as discussed in the section on electromagnetic enhancement).

The most common method used to synthesize both gold nanorods and nanostars is a seeded approach.<sup>131-133</sup> Gold seeds are synthesized then added to a solution containing gold salt, a reducing agent, and various shape-directing agents. Alternatively, a one-pot approach can be used in which gold nuclei form and are grown into larger structures in the same solution.<sup>134</sup> One common method uses an aqueous solution of ascorbic acid as reducing agent and CTAB and AgNO<sub>3</sub> as shape-directing agents. Other shape directing agents used for anisotropic gold nanoparticle synthesis include

polyvinylpyrrolidone (PVP)<sup>88,135</sup> and 2-[4-(2-hydroxyethyl)-1-piperazinyl] ethane-sulfonic acid (HEPES) buffer.<sup>136</sup>

In the following sections, we look at how interest has grown out of solid gold particles into particles with more complex nanostructures, featuring multiple hot-spots and multifunctionality, and their potential use in expanding our abilities to detect biomolecules.

### GOLD NANOSHELLS

The first syntheses of gold nanoshells,<sup>139</sup> involving gold shells covering cores of a dielectric material, are credited to Zhou et al for their synthesis of Au<sub>2</sub>S/Au core/shell particles<sup>140</sup> and later, to Oldenburg et al for their synthesis of silica/Au core/shell particles.<sup>141</sup> The significance of the latter synthesis was that it could be applied to particles of various sizes and compositions, thus opening up the study of the diagnostic potential of gold nanoshells. The synthesis involves binding gold seeds to a silica surface functionalized with amine groups, then adding the seeded particles to a solution containing gold salts to grow the seeds into a complete shell. By changing the core/shell ratio, the optical properties can be tuned.

In a recent work, Sauerbeck et al demonstrated that a partial shell results in greater second harmonic scattering (SHS) than a full shell, suggesting that the electromagnetic fields that lead to enhancement are greater when gold islands are present rather than a complete shell.<sup>142</sup> This effect may be due to the nanogaps between gold islands; as the spacing between islands decreases, the electric field in the gap increases until the gap closes and enhancement drops.

In the first cases of gold nanoshells, the core was used primarily as a template—a surface allowing for growth of a thin shell that exhibited interesting optical properties and a biocompatible surface for integration in diagnostic systems. Researchers quickly recognized, though, that using multiple materials could also be used to impart multiple functionalities. Since then, core-shell type particles with gold surfaces have been made incorporating properties such as magnetism, fluorescence, and Raman sensitivity.<sup>143</sup>

Multifunctional particles that include both a magnetic component and a plasmonic component have been investigated. These can be useful in situations where both particle movement and sensing are desired, such as purification and characterization of a biomolecule. Gold coating of small iron oxide particles is a common method,<sup>144,145</sup> since iron oxide particles less than 35 nm in diameter exhibit superparamagnetism.<sup>146</sup> The gold shell protects the iron oxide core and makes for simple functionalization chemistry, but more importantly, allows the particles to be used in applications that make use of the optical properties of nanogold, such as *in vivo* applications like contrast agents or applications combining magnetic separation and detection of biomolecules.

Gold shells have also been used to create nanogaps of a controlled size. Lim et al synthesized particles with a controllable interior gap by forming gold shells around gold cores using DNA to facilitate the formation of a nanogap

between the core and the shell.<sup>147</sup> By inserting Raman dyes into the ~1 nm nanogap, the researchers achieved quantitative and controllable SERS signals.

#### ANISOTROPIC GOLD NANOSHELLS

60

5 Particles with nanostructured surfaces are a next step in gold nanoparticle and nanoshell synthesis. In this section, the focus is on anisotropic and spiky particles with cores other than single small spherical gold seeds—the nanoparticles most commonly known as gold nanostars. As previously discussed, using  
10 alternative cores can infer new properties to the particles such as magnetism and fluorescence. Anisotropic shells can be formed on particles of different shapes and sizes; particles featuring multiple size scales can also lead to interesting new properties. In general, syntheses involve growing a gold shell  
15 around a core particle using variations of methods used to synthesize anisotropic particles. These particles exhibit interesting optical properties as the anisotropic points on the particles can create electromagnetic hot-spots, as described previously.

75

20 Similar methods can be used whether the core particle is gold, iron oxide, or other. Solid gold nanostructured particles are formed by growing branched structures on gold seeds or other gold nanoparticles. Alternatively, core-shell type particles can be nanostructured by either first forming a solid gold shell  
25 around a core of another material, or by binding gold seed particles to the core particle.

The most common strategy for anisotropic, spike growth is to reduce gold salts in the presence of a structure-directing agent. One common method involves reduction of  $\text{HAuCl}_4$  with  
30 ascorbic acid in the presence of CTAB and  $\text{AgNO}_3$ , which are involved in anisotropic structure formation. By varying the parameters, a number of different particle shapes can be formed—a similar method is in fact commonly used to form gold nanorods. Branched nanostructures are formed when  
35 ratio of seeds to gold ions is lowered.<sup>148</sup>

Small iron oxide particles have been coated with gold using this method to form gold nanostars with iron oxide cores.<sup>149-151</sup> Synthesis typically involves forming superparamagnetic iron oxide nanoparticles, followed by either the growth of a thin  
40 gold shell or gold seeding, then growing the shell using methods similar to those used to form anisotropic gold particles. This type of synthesis was reported where the researchers formed ultrathin gold shells (<2 nm) on  $\text{Fe}_3\text{O}_4$  nanoparticles in organic solvents, followed by anisotropic  
45 growth using a CTAB-based solution.<sup>149,150</sup> These anisotropic particles, with a final diameter of about 100 nm, were used for gyromagnetic imaging, which uses a rotating magnetic field gradient to vary the NIR scattering intensities; for applications such as contrast agents for biomedical imaging, this can result  
50 in images with less noise and thus better contrast.<sup>149,150</sup> In another example, researchers bound THPC-stabilized gold seeds to mercaptoundecanoic acid (MUA) terminated  $\text{Fe}_3\text{O}_4$  NPs, then used the CTAB-based method to grow spiked gold nanostars with iron oxide cores.<sup>151</sup> The resulting particles were  
55 used as recyclable catalysts for the reduction of  $\text{K}_3\text{Fe}(\text{CN})_6$ .

A CTAB-based growth method was also used to form spiky gold shells on larger particles, specifically block copolymer assemblies and polymer beads.<sup>152,153</sup> They first formed silver nanoparticles on the surface then used these as seeds in CTAB/Ag-solution based gold shell growth. This formed spiked shells with light adsorption reaching into the NIR range that varied with spike size. These were shown to give a single particle SERS signal with a low standard deviation compared with typical nanoparticle aggregates.

The sensitivity of the particle structure to the reagents is shown by researchers who used cetyltrimethylammonium chloride (CTAC) instead of cetyltrimethylammonium bromide (CTAB) and obtained nanoflowers with a different nanostructure than what has been seen using a CTAB-based method.<sup>154</sup> These gold nanoflowers were used as SERS tags in the detection of carcinoembryonic antigen (CEA) along with magnetic nanoparticles as supporting substrates.

Another procedure used to form nanostructured gold particles uses gold salts and polyvinylpyrrolidone (PVP) in DMF.<sup>91,155-157</sup> In this case, PVP acts as structure-directing agent and DMF is both solvent and reducing agent. The procedure has been used to grow spikes on gold nanowires,<sup>156</sup> gold nanorods,<sup>91</sup> and magnetite nanoparticles.<sup>157</sup> In the case of the magnetite particles, gold seeds were first grown on the surface, followed by spiked gold shell growth. All types of particles showed SERS enhancement. In the case of the gold/magnetite core-shell particles, used for protein magnetic separation, magnetically concentrating the particles led to the creation of SERS hot-spots as well.<sup>157</sup>

In most cases, spike growth is random and limited in the size of spikes that can be formed. Pedireddy et al demonstrated control over spike length using a PVP-based growth method on octahedral silver particles.<sup>158</sup> Spike length could be tuned between 10 and 130 nm by controlling the amount of gold salt and its injection rate throughout growth. Using electron energy loss spectroscopy (EELS), the researchers found that different spike lengths exhibited different optical responses.

Recent work has shown that surfactants are not necessary to form nanostructured particle surfaces. The main benefit of these methods is that the gold surface is relatively bare and can be more easily functionalized. Researchers used hydroquinone as a reducing agent to grow branches on gold seeds<sup>159</sup> and on gold-coated iron oxide.<sup>160</sup> Hydroxylamine can also act as a reducing agent in forming anisotropic particles when a shape-directing agent such as silver ions is present.<sup>161</sup> Another method uses triethanolamine in ethylene glycol to form clean gold nanoflowers, where the viscosity of the solution likely plays a role in directing anisotropic growth.<sup>162</sup>

Another approach to anisotropic particles involves controlled aggregation of small particles into larger, anisotropic clusters. One method uses HEPES buffer as a structure-directing agent.<sup>136,163</sup> The buffer acts as both a weak reducing agent and particle stabilizing agent, directing the growth of gold first into aggregates then into anisotropic nanoflowers. The size of the anisotropic branches can be controlled by varying the HEPES concentration. Researchers have demonstrated that the particles

can act as SERS tags with signals several orders of magnitude greater than seen with spherical particles.<sup>136</sup> They have also been functionalized with proteins for potential use as Raman-active tags for *in vivo* applications.<sup>163</sup> Others have used a similar approach based on the aggregation of small particles, but used superparamagnetic iron oxide nanoparticles coated with a thin gold shell to form the nanoclusters. Hydroxylamine directs gold reduction on the surface of particles, which then cluster together into nanoroses with diameters around 30 nm.<sup>164,165</sup> Researchers investigated the use of these particles for potential *in vivo* applications such as imaging, photothermal therapy, and drug delivery.

Table 1: Particles with nanostructured surfaces – method of synthesis and demonstrated application

	Reducing agent	Structure directing and/or stabilizing agent	Core	Demonstrated application	Ref
a, b	Ascorbic acid	CTAB and AgNO <sub>3</sub>	Fe <sub>3</sub> O <sub>4</sub> @Au core-shell NPs	Gyromagnetic imaging	149,150 *
c			Fe <sub>3</sub> O <sub>4</sub> NPs with THPC-stabilized AuNP seeds	Recyclable catalysts	151*
d			Polystyrene beads and block copolymers with Ag seeds	SERS	152,153
e	DMF	PVP	AuNPs, Au nanorods, Au nanowires	SERS	91,155,156 56
f			Fe <sub>3</sub> O <sub>4</sub> NPs with AuNP seeds	Magnetic separation of proteins and SERS	157*
g	Galvanic replacement	PVP	Silver octahedral particles	Enhanced electromagnetic properties	158*
h, i	Hydroquinone	sodium citrate	AuNPs, Fe <sub>3</sub> O <sub>4</sub> @Au core-shell NPs	Enhanced electromagnetic properties	159,160 *
j	Hydroxylamine	AgNO <sub>3</sub>	AuNPs	Enhanced electromagnetic properties	161*
k	Triethanolamine	Triethanolamine/ethylene glycol	-	SERS	162*
l	Hydroxylamine/HEPES	HEPES	AuNPs, agglomeration based	SERS	136*
m	HEPES	HEPES	-	non-toxic Raman tags	163*
n, o	Dextrose/hydroxylamine	Hydroxylamine	Fe <sub>3</sub> O <sub>4</sub> NPs	Cancer cell targeting, imaging, and therapy	164,165 *

\*Reference corresponding to figure

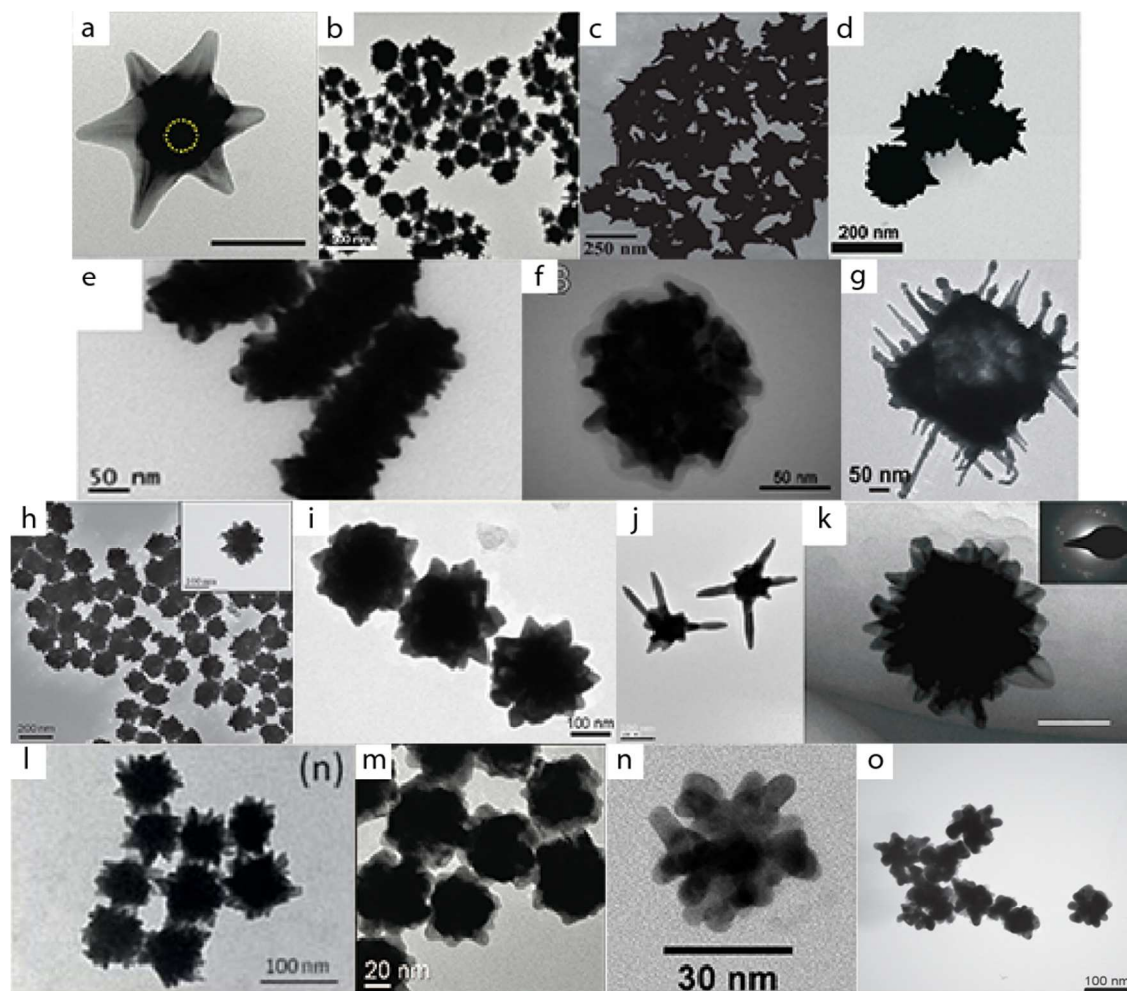


Figure 8: Examples of anisotropic particles from literature. Labels correspond to those in Table 1. All figures used with permission from listed reference

## ARTICLE

## Conclusions

Nanostructured and spiky gold is a valuable tool in biomolecule detection. Nanostructuring results in higher surface areas available for binding—a well-known fact within nanotechnology research—but also results in higher recognition efficiencies between biomolecules immobilized on nanostructured surfaces and target molecules than biomolecules immobilized on flat surfaces. As gold structures decrease in size, interesting plasmonic properties also appear that enhance signals of many optical detection methods. In particular, sharp tips and nanogaps act as electromagnetic hot-spots—areas of locally enhanced electromagnetic fields—that can enhance optical signals, often by orders of magnitude. Creating these gold nanostructures has been the subject of much creativity and effort; methods include chemical and topographical nanostructuring of planar and particle surfaces, involving nanogaps, sharp spikes, shells, and experimental and theoretical demonstrations of their use in biomolecule sensing. Despite the tremendous work in the area, challenges still remain in moving towards using these gold nanostructures in biosensing. The reproducibility issues seen with nanostructured gold SERS substrates in particular are common to most of the quantitative detection methods presented here; good solutions use simple methods of synthesis to make nanostructures with controlled size and spacing. This is true for both planar and particle substrates. In the case of anisotropic particle and shell synthesis, the commonly used gold reduction methods are notoriously sensitive to multiple factors, making reproducible syntheses a challenge. Another challenge in these syntheses is the presence of stabilizing groups that typically must be displaced before an analyte can be detected. The past few years have seen many innovative approaches to these challenges and there is little doubt that continued work will solve them.

Spiky gold is a tool to tackle two of the main challenges associated with biosensing: ensuring that enough biomolecules are bound to the surface to be detected and that each biomolecule bound results in a high enough signal to be detected. Combining nanostructured gold with materials that infer other functionalities may provide the means to tackle others. An example of this is using magnetic cores within spiky gold shells to combine magnetic separation with biosensing. This approach may help when trying to detect analytes at low concentrations; the particles could be dispersed in a larger volume to bind the analyte then magnetically concentrated before detecting the analyte.

Continued work on understanding the hot-spot effect, the optimal structures, and methods to synthesize them simply and

reproducibly will greatly benefit the field of highly sensitive biomolecule detection.

## Notes and references

<sup>a</sup> Sorbonne Universités, UPMC University Paris 6, UMR CNRS 7197, Laboratoire de Réactivité de Surface, F75005 Paris, France

<sup>b</sup> UMR CNRS 7197, Laboratoire de Réactivité de Surface, F75005 Paris, France

<sup>c</sup> Department of Chemical Engineering, University of Waterloo, 200 University Avenue W, Waterloo, Ontario, Canada, N2L 3G1

<sup>d</sup> Waterloo Institute for Nanotechnology, University of Waterloo, 200 University Avenue W, Waterloo, Ontario, Canada, N2L 3G1

1. A. P. F. Turner, *Chem. Soc. Rev.*, 2013, **42**, 3184–3196.
2. K. B. Cederquist and S. O. Kelley, *Current Opinion in Chemical Biology*, 2012, **16**, 415–421.
3. E. Katz and I. Willner, *Angew. Chem. Int. Ed.*, 2004, **43**, 6042–6108.
4. C. M. Niemeyer, *Angew. Chem. Int. Ed.*, 2001, **40**, 4128–4158.
5. E. C. Dreaden, A. M. Alkilany, X. Huang, C. J. Murphy, and M. A. El-Sayed, *Chem. Soc. Rev.*, 2012, **41**, 2740–2779.
6. S. Eustis and M. A. El-Sayed, *ChemInform*, 2006, **37**.
7. M. A. Garcia, *Journal of Physics D: Applied Physics*, 2011, **45**, 389501.
8. S. Lal, N. K. Grady, J. Kundu, C. S. Levin, J. B. Lassiter, and N. J. Halas, *Chem. Soc. Rev.*, 2008, **37**, 898–911.
9. B. Sepúlveda, P. C. Angelomé, L. M. Lechuga, and L. M. Liz-Marzán, *Nano Today*, 2009, **4**, 244–251.
10. C. Hrelescu, T. K. Sau, A. L. Rogach, F. Jäckel, and J. Feldmann, *Appl. Phys. Lett.*, 2009, **94**, 153113.
11. A. Li and S. Li, *Nanoscale*, 2014, **6**, 12921–12928.
12. S. R. Beeram and F. P. Zamborini, *J. Am. Chem. Soc.*, 2009, **131**, 11689–11691.
13. L. Feuz, M. P. Jonsson, and F. Höök, *Nano Lett.*, 2012, **12**, 873–879.
14. P. K. Jain, X. Huang, I. H. El-Sayed, and M. A. El-Sayed, *Plasmonics*, 2007, **2**, 107–118.
15. A. J. Haes and R. P. Van Duyne, *Anal. Bioanal. Chem.*, 2004, **379**, 920–930.
16. D. Ciialla, A. März, R. Böhme, F. Theil, K. Weber, M. Schmitt, and J. Popp, *Anal. Bioanal. Chem.*, 2012, **403**, 27–54.
17. J. P. Camden, J. A. Dieringer, J. Zhao, and R. P. Van Duyne, *Acc. Chem. Res.*, 2008, **41**, 1653–1661.
18. M. Osawa, in *Near-Field Optics and Surface Plasmon Polaritons*, Springer Berlin Heidelberg, Berlin, Heidelberg, 2006, vol. 81, pp. 163–187.
19. C. M. Pradier, M. Salmain, and S. Boujday, in *Biointerface Characterization by Advanced IR Spectroscopy*, Elsevier, 2011, pp. 167–216.
20. D. Darvill, A. Centeno, and F. Xie, *Phys. Chem. Chem. Phys.*, 2013, **15**, 15709–15726.
21. P. Gong and R. Levicky, *Proceedings of the National Academy of Sciences*, 2008, **105**, 5301–5306.
22. D. Irving, P. Gong, and R. Levicky, *J. Phys. Chem. B*, 2010, **114**, 7631–7640.
23. A. W. Peterson, *Nucleic Acids Research*, 2001, **29**, 5163–5168.
24. K. Castelino, B. Kannan, and A. Majumdar, *Langmuir*, 2005, **21**, 1956–1961.
25. A. Kira, H. Kim, and K. Yasuda, *Langmuir*, 2009, **25**, 1285–1288.
26. H. D. Hill, J. E. Millstone, M. J. Banholzer, and C. A. Mirkin, *ACS Nano*, 2009, **3**, 418–424.

27. L. Soleymani, Z. Fang, X. Sun, H. Yang, B. J. Taft, E. H. Sargent, and S. O. Kelley, *Angewandte Chemie*, 2009, **121**, 8609–8612.
28. X. Bin, E. H. Sargent, and S. O. Kelley, *Anal. Chem.*, 2010, **82**, 5928–5931.
29. L. Soleymani, Z. Fang, E. H. Sargent, and S. O. Kelley, *Nature Nanotech*, 2009, **4**, 844–848.
30. I. Ivanov, J. Stojcic, A. Stanimirovic, E. Sargent, R. K. Nam, and S. O. Kelley, *Anal. Chem.*, 2013, **85**, 398–403.
31. E. Vasilyeva, B. Lam, Z. Fang, M. D. Minden, E. H. Sargent, and S. O. Kelley, *Angew. Chem. Int. Ed.*, 2011, **50**, 4137–4141.
32. L. Soleymani, Z. Fang, B. Lam, X. Bin, and E. Vasilyeva, *ACS Nano*, 2011, **5**, 3360–3366.
33. F. Li, X. Han, and S. Liu, *Biosens. Bioelectron.*, 2011, **26**, 2619–2625.
34. L. Shi, Z. Chu, Y. Liu, W. Jin, and X. Chen, *Biosens. Bioelectron.*, 2013, **49**, 184–191.
35. C. Zanardi, C. Baldoli, E. Licandro, F. Terzi, and R. Seeber, *J. Nanopart. Res.*, 2012, **14**, 1148.
36. L. Wang, X. Chen, X. Wang, X. Han, S. Liu, and C. Zhao, *Biosens. Bioelectron.*, 2011, **30**, 151–157.
37. T. H. M. Kjällman, H. Peng, C. Soeller, and J. Travas-Sejdic, *Anal. Chem.*, 2008, **80**, 9460–9466.
38. B. Lu, M. R. Smyth, and R. Okennedy, *Analyst*, 1996, **121**, R29–R32.
39. Y. Jung, J. Y. Jeong, and B. H. Chung, *Analyst*, 2008, **133**, 697–701.
40. P. Sen, S. Yamaguchi, and T. Tahara, *J. Phys. Chem. B*, 2008, **112**, 13473–13475.
41. C. Lahari, L. S. Jasti, N. W. Fadnavis, K. Sontakke, G. Ingavle, S. Deokar, and S. Ponrathnam, *Langmuir*, 2010, **26**, 1096–1106.
42. S. Boujday, A. Bantegnie, E. Briand, P. G. Marnet, M. Salmain, and C. M. Pradier, *J. Phys. Chem. B*, 2008, **112**, 6708–6715.
43. A. Makaraviciute and A. Ramanaviciene, *Biosens. Bioelectron.*, 2013, **50**, 460–471.
44. A. M. Reed and S. J. Metallo, *Langmuir*, 2010, **26**, 18945–18950.
45. Y. H. Tan, M. Liu, B. Nolting, J. G. Go, J. Gervay-Hague, and G.-Y. Liu, *ACS Nano*, 2008, **2**, 2374–2384.
46. E. Briand, M. L. Salmain, J.-M. Herry, H. Perrot, C. Comp re, and C.-M. Pradier, *Biosens. Bioelectron.*, 2006, **22**, 440–448.
47. J. N. Ngunjiri, D. J. Stark, T. Tian, K. A. Briggman, and J. C. Garmo, *Anal. Bioanal. Chem.*, 2013, **405**, 1985–1993.
48. H. Tokuhisa, J. Liu, K. Omori, M. Kanesato, K. Hiratani, and L. A. Baker, *Langmuir*, 2009, **25**, 1633–1637.
49. R. Carbone, M. De Marni, A. Zanardi, S. Vinati, E. Barborini, L. Fornasari, and P. Milani, *Anal. Biochem.*, 2009, **394**, 7–12.
50. V. Mani, B. V. Chikkaveeraiah, V. Patel, J. S. Gutkind, and J. F. Rusling, *ACS Nano*, 2009, **3**, 585–594.
51. B. S. Munge, A. L. Coffey, J. M. Doucette, B. K. Somba, R. Malhotra, V. Patel, J. S. Gutkind, and J. F. Rusling, *Angew. Chem. Int. Ed.*, 2011, **50**, 7915–7918.
52. E. E. Bedford, J. Spadavecchia, C.-M. Pradier, and F. X. Gu, *Macromol. Biosci.*, 2012, **12**, 724–739.
53. J. Homola, *Chem. Rev.*, 2008, **108**, 462–493.
54. M. C. Estevez, M. A. Otte, B. Sepúlveda, and L. M. Lechuga, *Anal. Chim. Acta*, 2014, **806**, 55–73.
55. N. J. Halas, S. Lal, S. Link, W.-S. Chang, D. Natelson, J. H. Hafner, and P. Nordlander, *Adv. Mater.*, 2012, **24**, 4842–4877.
56. G. P. Acuna, F. M. Möller, P. Holzmeister, S. Beater, B. Lalkens, and P. Tinnefeld, *Science*, 2012, **338**, 506–510.
57. F. Hao, C. L. Nehl, J. H. Hafner, and P. Nordlander, *Nano Lett.*, 2007, **7**, 729–732.
58. A. Kinkhabwala, Z. Yu, S. Fan, Y. Avlasevich, K. M. U. Ilen, and W. E. Moerner, *Nature Photonics*, 2009, **3**, 654–657.
59. C. A. Mirkin, R. L. Letsinger, R. C. Mucic, and J. J. Storhoff, *Nature*, 1996, **382**, 607–609.
60. D. Aili, R. Selegård, L. Baltzer, K. Enander, and B. Liedberg, *Small*, 2009, **5**, 2445–2452.
61. X. Liu, Y. Wang, P. Chen, Y. Wang, J. Zhang, D. Aili, and B. Liedberg, *Anal. Chem.*, 2014, **86**, 2345–2352.
62. L. A. Lyon, M. D. Musick, and M. J. Natan, *Anal. Chem.*, 1998, **70**, 5177–5183.
63. E. Hutter, S. Cha, J.-F. Liu, J. Park, J. Yi, J. H. Fendler, and D. Roy, *J. Phys. Chem. B*, 2001, **105**, 8–12.
64. X. Yang, Q. Wang, K. Wang, W. Tan, and H. Li, *Biosens. Bioelectron.*, 2007, **22**, 1106–1110.
65. J. Spadavecchia, S. Casale, S. Boujday, and C.-M. Pradier, *Colloids and Surfaces B: Biointerfaces*, 2012, **100**, 1–8.
66. J. S. Mitchell, Y. Wu, C. J. Cook, and L. Main, *Anal. Biochem.*, 2005, **343**, 125–135.
67. G. A. J. Besselink, R. P. H. Kooyman, P. J. H. J. van Os, G. H. M. Engbers, and R. B. M. Schasfoort, *Anal. Biochem.*, 2004, **333**, 165–173.
68. J. Wang and H. S. Zhou, *Anal. Chem.*, 2008, **80**, 7174–7178.
69. A. R. Halpern, J. B. Wood, Y. Wang, and R. M. Corn, *ACS Nano*, 2013.
70. S. Ko, T. J. Park, H.-S. Kim, J.-H. Kim, and Y.-J. Cho, *Biosens. Bioelectron.*, 2009, **24**, 2592–2597.
71. E. Hutter, J. H. Fendler, and D. Roy, *J. Phys. Chem. B*, 2001, **105**, 11159–11168.
72. J. Jung, K. Na, J. Lee, K.-W. Kim, and J. Hyun, *Anal. Chim. Acta*, 2009, **651**, 91–97.
73. S. Gao, N. Koshizaki, H. Tokuhisa, E. Koyama, T. Sasaki, J.-K. Kim, J. Ryu, D.-S. Kim, and Y. Shimizu, *Adv. Funct. Mater.*, 2010, **20**, 78–86.
74. W. P. Hu, S.-J. Chen, K.-T. Huang, J. H. Hsu, W. Y. Chen, G. L. Chang, and K.-A. Lai, *Biosens. Bioelectron.*, 2004, **19**, 1465–1471.
75. T. Kawaguchi, D. R. Shankaran, S. J. Kim, K. Matsumoto, K. Toko, and N. Miura, *Sens. Actuator B-Chem.*, 2008, **133**, 467–472.
76. R. Gordon, D. Sinton, K. L. Kavanagh, and A. G. Brolo, *Acc. Chem. Res.*, 2008, **41**, 1049–1057.
77. Y. Wang, B. Yan, and L. Chen, *Chem. Rev.*, 2012, **113**, 1391–1428.
78. M. Fleischmann, P. J. Hendra, and A. J. McQuillan, *Chemical Physics Letters*, 1974, **26**, 163–166.
79. H. Ko, S. Singamaneni, and V. V. Tsukruk, *Small*, 2008, **4**, 1576–1599.
80. M. Moskovits, *J. Raman Spectrosc.*, 2005, **36**, 485–496.
81. P. J. Schuck, D. P. Fromm, A. Sundaramurthy, G. S. Kino, and W. E. Moerner, *Phys. Rev. Lett.*, 2005, **94**, 017402.
82. L. Gunnarsson, T. Rindzevicius, J. Prikulis, B. Kasemo, M. Käll, S. Zou, and G. C. Schatz, *J. Phys. Chem. B*, 2005, **109**, 1079–1087.
83. C. E. Talley, J. B. Jackson, C. Oubre, N. K. Grady, C. W. Hollars, S. M. Lane, T. R. Huser, P. Nordlander, and N. J. Halas, *Nano Lett.*, 2005, **5**, 1569–1574.
84. W. Li, P. H. C. Camargo, X. Lu, and Y. Xia, *Nano Lett.*, 2009, **9**, 485–490.
85. P. F. Liao and A. Wokaun, *The Journal of Chemical Physics*, 1982, **76**, 751–752.
86. C. Hrelescu, T. K. Sau, A. L. Rogach, F. Jäckel, G. Laurent, L. Douillard, and F. Charra, *Nano Lett.*, 2011, **11**, 402–407.
87. M. E. Stewart, C. R. Anderton, L. B. Thompson, J. Maria, S. K. Gray, J. A. Rogers, and R. G. Nuzzo, *Chem. Rev.*, 2008, **108**, 494–521.
88. S. Barbosa, A. Agrawal, L. Rodríguez-Lorenzo, I. Pastoriza-Santos, R. A. Alvarez-Puebla, A. Kornowski, H. Weller, and L. M. Liz-Marzán, *Langmuir*, 2010, **26**, 14943–14950.
89. E. Nalbant Esenturk and A. R. Hight Walker, *J. Raman Spectrosc.*, 2009, **40**, 86–91.
90. X.-M. Lin, Y. Cui, Y.-H. Xu, B. Ren, and Z.-Q. Tian, *Anal. Bioanal. Chem.*, 2009, **394**, 1729–1745.
91. P. Aldeanueva-Potel, E. Carbó-Argibay, N. Pazos-Pérez, S. Barbosa, I. Pastoriza-Santos, R. A. Alvarez-Puebla, and L. M. Liz-Marzán, *ChemPhysChem*, 2012, **13**, 2561–2565.
92. L. Osinkina, T. Lohmüller, F. Jäckel, and J. Feldmann, *J. Phys. Chem. C*, 2013, **117**, 22198–22202.
93. F. Le, D. W. Brandl, Y. A. Urzhumov, H. Wang, J. Kundu, N. J. Halas, J. Aizpurua, and P. Nordlander, *ACS Nano*, 2008, **2**, 707–718.
94. K. Aslan, I. Gryczynski, J. Malicka, E. Matveeva, J. R. Lakowicz, and C. D. Geddes, *Current Opinion in Biotechnology*, 2005, **16**, 55–62.

95. R. Luchowski, T. Shtoyko, E. Matveeva, P. Sarkar, J. Borejdo, Z. Gryczynski, and I. Gryczynski, *Appl Spectrosc*, 2010, **64**, 578–583.
96. R. Luchowski, E. Matveeva, T. Shtoyko, P. Sarkar, L. Patsenker, O. Klochko, E. Terpetschnig, J. Borejdo, I. Akopova, Z. Gryczynski, and I. Gryczynski, *Curr. Pharm. Biotech.*, 2010, **11**, 96–102.
97. K. Aslan, M. Wu, J. R. Lakowicz, and C. D. Geddes, *J. Am. Chem. Soc.*, 2007, **129**, 1524–1525.
98. J. C. Love, L. A. Estroff, J. K. Kriebel, R. G. Nuzzo, and G. M. Whitesides, *Chem. Rev.*, 2005, **105**, 1103–1170.
99. K. L. Prime and G. M. Whitesides, *Science*, 1991, **252**, 1164–1167.
100. T. Wink, S. J. van Zuilen, A. Bult, and W. P. van Bennekom, *Analyst*, 1997, **122**, 43R–50R.
101. S. Boujday, R. Briandet, M. Salmain, J.-M. Herry, P.-G. Marnet, M. Gautier, and C.-M. Pradier, *Microchimica Acta*, 2008, **163**, 203–209.
102. E. Briand, C. Gu, S. Boujday, M. Salmain, J. M. Herry, and C. M. Pradier, *Surf. Sci.*, 2007, **601**, 3850–3855.
103. E. E. Bedford, S. Boujday, V. Humblot, F. X. Gu, and C.-M. Pradier, *Colloids and Surfaces B: Biointerfaces*, 2014, **116**, 489–496.
104. V. Lebec, J. Landoulsi, S. Boujday, C. Poleunis, C. M. Pradier, and A. Delcorte, *J. Phys. Chem. C*, 2013, **117**, 11569–11577.
105. C. Vericat, M. E. Vela, G. Benitez, P. Carro, and R. C. Salvarezza, *Chem. Soc. Rev.*, 2010, **39**, 1805–1834.
106. R. K. Smith, P. A. Lewis, and P. S. Weiss, *Prog. Surf. Sci.*, 2004, **75**, 1–68.
107. K. Tamada, M. Hara, H. Sasabe, and W. Knöll, *Langmuir*, 1997, **13**, 1558–1566.
108. N. J. Brewer and G. J. Leggett, *Langmuir*, 2004, **20**, 4109–4115.
109. E. Ostuni, L. Yan, and G. M. Whitesides, *Colloids and Surfaces B: Biointerfaces*, 1999, **15**, 3–30.
110. K. E. Nelson, L. Gamble, L. S. Jung, M. S. Boeckl, E. Naemi, S. L. Gollledge, T. Sasaki, D. G. Castner, C. T. Campbell, and P. S. Stayton, *Langmuir*, 2001, **17**, 2807–2816.
111. D. Samanta and A. Sarkar, *Chem. Soc. Rev.*, **40**, 2567–2592.
112. E. A. Josephs and T. Ye, *J. Am. Chem. Soc.*, 2010, **132**, 10236–10238.
113. T. M. Herne and M. J. Tarlov, *J. Am. Chem. Soc.*, 1997, **119**, 8916–8920.
114. C.-Y. Lee, P. Gong, G. M. Harbers, D. W. Grainger, D. G. Castner, and L. J. Gamble, *Anal. Chem.*, 2006, **78**, 3316–3325.
115. J. D. Driskell, R. J. Lipert, and M. D. Porter, *J. Phys. Chem. B*, 2006, **110**, 17444–17451.
116. A.-L. Morel, R.-M. Volmant, C. Méthivier, J.-M. Krafft, S. Boujday, and C.-M. Pradier, *Colloids and Surfaces B: Biointerfaces*, 2010, **81**, 304–312.
117. M. Ben Haddada, J. Blanchard, S. Casale, J.-M. Krafft, A. Vallée, C. Méthivier, and S. Boujday, *Gold Bull*, 2013, **46**, 335–341.
118. A. Wei, *Chem. Commun. (Camb.)*, 2006, 1581–1591.
119. M. Eichler, V. Katzur, L. Scheideler, M. Haupt, J. Geis-Gerstorfer, G. Schmalz, S. Ruhl, R. Muller, and F. Rupp, *Biomaterials*, **32**, 9168–9179.
120. D. Mercier, S. Boujday, C. Annabi, R. Villanneau, C.-M. Pradier, and A. Proust, *J. Phys. Chem. C*, 2012, **116**, 13217–13224.
121. X. Yu, B. Munge, V. Patel, and G. Jensen, *J. Am. Chem. Soc.*, 2006, **128**, 11199–11205.
122. J. C. Hulteen and R. P. Van Duyne, *Journal of Vacuum Science & Technology A: Vacuum, Surfaces, and Films*, 1995, **13**, 1553–1558.
123. Amanda J Haes, Lei Chang, A. William L Klein, Richard P Van Duyne, *J. Am. Chem. Soc.*, 2005, **127**, 2264–2271.
124. C. L. Haynes and R. P. Van Duyne, *J. Phys. Chem. B*, 2003, **107**, 7426–7433.
125. W. Ye, J. Yan, Q. Ye, and F. Zhou, *J. Phys. Chem. C*, 2010, **114**, 15617–15624.
126. W. Ye, D. Wang, H. Zhang, F. Zhou, and W. Liu, *Electrochimica Acta*, 2010, **55**, 2004–2009.
127. J. Wang, G. Duan, Y. Li, G. Liu, Z. Dai, H. Zhang, and W. Cai, *Langmuir*, 2013, **29**, 3512–3517.
128. N. L. Rosi and C. A. Mirkin, *Chem. Rev.*, 2005, **105**, 1547–1562.
129. M.-C. Daniel and D. Astruc, *Chem. Rev.*, 2004, **104**, 293–346.
130. P. Zhao, N. Li, and D. Astruc, *Coordination Chemistry Reviews*, 2013, **257**, 638–665.
131. S. E. Lohse and C. J. Murphy, *Chem. Mater.*, 2013, **25**, 1250–1261.
132. C. J. Murphy, T. K. Sau, A. M. Gole, C. J. Orendorff, J. Gao, L. Gou, S. E. Hunyadi, and T. Li, *J. Phys. Chem. B*, 2005, **109**, 13857–13870.
133. M. Treguer-Delapierre, J. Majimel, S. Mornet, E. Duguet, and S. Ravaine, *Gold Bull*, 2008, **41**, 195–207.
134. A. Guerrero-Martínez, S. Barbosa, I. Pastoriza-Santos, and L. M. Liz-Marzán, *Current Opinion in Colloid & Interface Science*, 2011, **16**, 118–127.
135. P. Senthil Kumar, I. Pastoriza-Santos, B. Rodríguez-González, F. Javier García de Abajo, and L. M. Liz-Marzán, *Nanotechnology*, 2008, **19**, 015606.
136. G. Maiorano, L. Rizzello, M. A. Malvindi, S. S. Shankar, L. Martiradonna, A. Falqui, R. Cingolani, and P. P. Pompa, *Nanoscale*, 2011, **3**, 2227–2232.
137. Z. Zhong, S. Patskovskyy, P. Bouvrette, J. H. T. Luong, and A. Gedanken, *J. Phys. Chem. B*, 2004, **108**, 4046–4052.
138. C. L. Nehl, H. Liao, and J. H. Hafner, *Nano Lett.*, 2006, **6**, 683–688.
139. L. R. Hirsch, A. M. Gobin, A. R. Lowery, F. Tam, R. A. Drezek, N. J. Halas, and J. L. West, *Nanoscale*, 2013, **5**, 2589–2599.
140. H. Zhou, I. Honma, H. Komiyama, and J. Haus, *Phys. Rev. B*, 1994, **50**, 12052–12056.
141. S. J. Oldenburg, R. D. Averitt, S. L. Westcott, and N. J. Halas, *Chemical Physics Letters*, 1998, **288**, 243–247.
142. C. Sauerbeck, M. Haderlein, B. Schürer, B. Braunschweig, W. Peukert, and R. N. Klupp Taylor, *ACS Nano*, 2014, **8**, 3088–3096.
143. N. C. Bigall, W. J. Parak, and D. Dorfs, *Nano Today*, 2012, **7**, 282–296.
144. C. S. Levin, C. Hofmann, T. A. Ali, A. T. Kelly, E. Morosan, P. Nordlander, K. H. Whitmire, and N. J. Halas, *ACS Nano*, 2009, **3**, 1379–1388.
145. H. Zhang, M. H. Harpster, W. C. Wilson, and P. A. Johnson, *Langmuir*, 2012, **28**, 4030–4037.
146. D. J. Dunlop, *Science*, 1972, **176**, 41–43.
147. D.-K. Lim, K.-S. Jeon, J.-H. Hwang, H. Kim, S. Kwon, Y. D. Suh, and J.-M. Nam, *Nature Nanotech*, 2011, **6**, 452–460.
148. T. K. Sau and C. J. Murphy, *J. Am. Chem. Soc.*, 2004, **126**, 8648–8649.
149. Q. Wei, H.-M. Song, A. P. Leonov, J. A. Hale, D. Oh, Q. K. Ong, K. Ritchie, and A. Wei, *J. Am. Chem. Soc.*, 2009, **131**, 9728–9734.
150. H.-M. Song, Q. Wei, Q. K. Ong, and A. Wei, *ACS Nano*, 2010, **4**, 5163–5173.
151. X. Miao, T. Wang, F. Chai, X. Zhang, C. Wang, and W. Sun, *Nanoscale*, 2011, **3**, 1189.
152. B. L. Sanchez-Gaytan and S.-J. Park, *Langmuir*, 2010, **26**, 19170–19174.
153. B. L. Sanchez-Gaytan, P. Swanglap, T. J. Lamkin, R. J. Hickey, Z. Fakhraei, S. Link, and S.-J. Park, *J. Phys. Chem. C*, 2012, **116**, 10318–10324.
154. C. Song, L. Min, N. Zhou, Y. Yang, B. Yang, L. Zhang, S. Su, and L. Wang, *RSC Adv.*, 2014, **4**, 41666–41669.
155. I. Pastoriza-Santos and L. M. Liz-Marzán, *Adv. Funct. Mater.*, 2009, **19**, 679–688.
156. N. Pazos-Pérez, S. Barbosa, L. Rodríguez-Lorenzo, P. Aldeanueva-Potel, J. Pérez-Juste, I. Pastoriza-Santos, R. A. Alvarez-Puebla, and L. M. Liz-Marzán, *J. Phys. Chem. Lett.*, 2010, **1**, 24–27.
157. P. Quaresma, I. Osório, G. Dória, P. A. Carvalho, A. Pereira, J. Langer, J. P. Araújo, I. Pastoriza-Santos, L. M. Liz-Marzán, R. Franco, P. V. Baptista, and E. Pereira, *RSC Adv.*, 2013, **4**, 3659.
158. S. Pedireddy, A. Li, M. Bosman, I. Y. Phang, S. Li, and X. Y. Ling, *J. Phys. Chem. C*, 2013, **117**, 16640–16649.
159. J. Li, J. Wu, X. Zhang, Y. Liu, D. Zhou, H. Sun, H. Zhang, and B. Yang, *J. Phys. Chem. C*, 2011, **115**, 3630–3637.

## Journal Name

160. H. Zhou, J.-P. Kim, J. H. Bahng, N. A. Kotov, and J. Lee, *Adv. Funct. Mater.*, 2013, **24**, 1439–1448.
161. H. Yuan, W. Ma, C. Chen, J. Zhao, J. Liu, H. Zhu, and X. Gao, *Chem. Mater.*, 2007, **19**, 1592–1600.
162. Y. Jiang, X.-J. Wu, Q. Li, J. Li, and D. Xu, *Nanotechnology*, 2011, **22**, 385601.
163. J. Xie, Q. Zhang, J. Y. Lee, and D. I. C. Wang, *ACS Nano*, 2008, **2**, 2473–2480.
164. L. L. Ma, M. D. Feldman, J. M. Tam, A. S. Paranjape, K. K. Cheruku, T. A. Larson, J. O. Tam, D. R. Ingram, V. Paramita, J. W. Villard, J. T. Jenkins, T. Wang, G. D. Clarke, R. Asmis, K. Sokolov, B. Chandrasekar, T. E. Milner, and K. P. Johnston, *ACS Nano*, 2009, **3**, 2686–2696.
165. C. Li, T. Chen, I. Ocoy, G. Zhu, E. Yasun, M. You, C. Wu, J. Zheng, E. Song, C. Z. Huang, and W. Tan, *Adv. Funct. Mater.*, 2013, **24**, 1772–1780.